X-ray resonant Raman scattering in NiO: Resonant enhancement of the charge-transfer excitations

C.-C. Kao, W. A. L. Caliebe, and J. B. Hastings

National Synchrotron Light Source, Brookhaven National Laboratory, Upton, New York 11973

J.-M. Gillet

Department of Material Science, Universite de Marne la Vallee, 93166 Noisy le Grand Cedex, France

(Received 13 September 1996)

An energy loss feature with energy transfer close to the anion-to-cation charge-transfer energy of NiO is observed in the inelastic-x-ray-scattering spectrum as the incident x-ray energy is tuned through the Ni K absorption edge of NiO. The inelastic-scattering cross section shows large resonant enhancement and strong incident energy dependence. These observations are interpreted using a configuration-interaction cluster model of NiO. [S0163-1829(96)04548-1]

The cross section for inelastic x-ray scattering is derived from the photon-electron interaction Hamiltonian. Within the nonrelativistic limit, the cross section contains matrix elements arising from perturbation treatment of either the $\mathbf{A}^2$ term in first order or the $\mathbf{p} \cdot \mathbf{A}$ term in second order.[1] The contribution of the $\mathbf{p} \cdot \mathbf{A}$ term to the total cross section can be significantly enhanced, in principle, by exploiting the resonant conditions in the matrix elements, i.e., by tuning the incident photon energy near an absorption threshold of the sample. Experimentally, large resonant enhancement of the inelastic-x-ray-scattering cross section was observed by Sparks[2] and is usually referred to as x-ray resonant Raman scattering (XRRS) to distinguish it from inelastic-scattering processes originating from the $\mathbf{A}^2$ term in the interaction Hamiltonian. The advent of synchrotron radiation as an intense and tunable x-ray source has made it possible to study the energy dependence of XRRS in greater detail and with increasingly better energy resolution. As a result, many interesting threshold phenomena were revealed, and applications of XRRS developed.[3]

However, limited by the incident photon flux, most of the aforementioned XRRS experiments involved resonant Raman processes in which both the intermediate states and the final states correspond to localized core electron excitations. High-energy-resolution study of resonant Raman processes in which the final states correspond to elementary excitations of the conduction electrons or the valence electrons in condensed matter has become possible only recently with the development of high-flux insertion devices. An important class of experiment is the recent high-energy resolution study of the excitation energy dependence in soft-x-ray emission spectroscopy.[4] For wideband solids, such as Si and diamond, strong excitation energy and orientation dependence of the valence-band emission spectra were observed and interpreted using the one-electron band structure of the material. The origin of these effects was attributed to the existence of temporal and spatial coherence in the x-ray absorption and the subsequent emission process.[5] On the other hand, for narrow-band solids, such as transition-metal and rare-earther compounds, the excitation energy dependence is usually interpreted in terms of multielectron satel-lites or correlation effects and is believed to provide unique information on the electronic structure of these important materials. For example, recent theoretical investigation has shown that resonant excitation of the Cu $3d \rightarrow 2p$ emission spectra is particularly sensitive to the electronic states due to the existence of apical oxygen in La_2CuO_4 and high-temperature Cu superconductors.[6] However, more high-resolution experimental data are needed to verify these predictions.

In this work, we report the results of a hard-x-ray high-resolution XRRS study of NiO, one of the prototypical Mott-Hubbard systems. Inelastic-x-ray-scattering spectra near the NiO valence-band emission energy were measured as the incident photon energy scanned through the Ni K absorption edge. A different spectral feature, which is not observed for incident energies far away from the absorption edge, appears in the inelastic-scattering spectra in addition to the valence-band emission spectrum. While the average energy of the valence-band emission spectrum remains constant, the average energy of this feature disperses linearly with the incident photon energy. The average energy transfer of this feature is about 6.5 eV, which is close to the recently reported anion-to-cation charge-transfer energy of NiO.[7,8] It should be noted that the charge-transfer energy is usually indirectly deduced from the results of a combination of valence-band photo-emission and inverse photoemission measurements[8] or other core electron spectroscopies.[7] Furthermore, by comparing with electron energy-loss spectroscopy measurements,[9] the inelastic-scattering cross section for the excitation of this feature shows very large resonant enhancement. The on-resonant cross section is estimated to be on the order of 100 times larger than the off-resonant cross section. This large enhancement is very important because high-energy-resolution inelastic x-ray scattering is still severely limited by the incident photon flux even with new synchrotron radiation sources.

The experiment was performed at the X21 hybrid wiggler beamline at the National Synchrotron Light Source. The beamline consists of a horizontal focusing Si(220) mono-chromator and a spherically bent backscattering analyzer.[10] At 8 keV, the energy resolution of the monochromator is
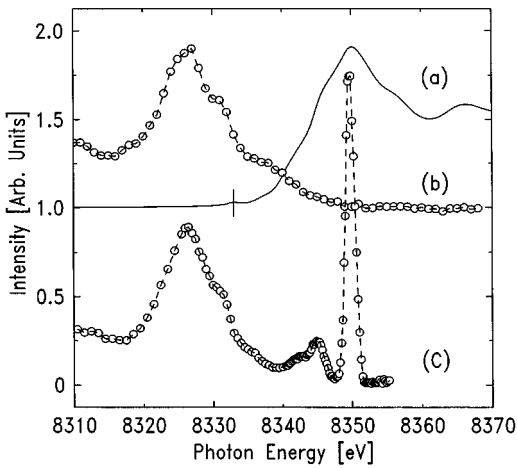
FIG. 1. (a) Ni K absorption spectrum of NiO. (b) Normal valence-band x-ray-emission spectrum of NiO. (c) Resonant inelastic x-ray-scattering spectrum of NiO obtained with the incident photon energy tuned to the main peak of the absorption spectrum (a).

about 0.7 eV, the focused incident beam size at the sample is about 0.2 mm in the horizontal and 10 mm in the vertical, and the photon flux is about 2×10^{11} photon/sec at 100 mA ring current. For the nonresonant measurements, a Si(444) analyzer crystal was used so that both the incident and scattered photon energies are a few hundred eV below the Ni K absorption edge to reduce sample absorption. The total energy resolution of the nonresonant measurements was 1.0 eV. For the resonant measurements, since the photon energy is determined by the Ni K absorption edge energy, a Si(551) analyzer crystal was used to improve the energy resolution. The total energy resolution of the resonant measurements was 1.5 eV. The sample used in the experiment was a single crystal NiO disk oriented in the (001) direction. All spectra reported here were measured at the scattering angle $\theta = 30°$ and in the horizontal plane. The wave-vector transfer Q, defined as $4\pi \sin(\theta/2)/\lambda$, was also in the (001) direction.

Curve (a) in Fig. 1 shows the Ni K edge absorption spectrum of a powdered NiO sample. The spectrum is characterized by a weak pre-edge peak, marked by the short vertical line, and a series of small absorption features leading up to the main absorption peak, centered around 8350 eV. The pre-edge peak, located at 8333 eV, is usually assigned to the $1s \rightarrow 3d$ transition, while the main peak and the absorption features between the pre-edge peak and the main peak are assigned to transitions from the Ni $1s$ core state to Ni-$4p$-like states.[11] Also shown in Fig. 1, curve (b), is the normal x-ray emission spectrum corresponding to the decay of the valence electrons of NiO into the Ni $1s$ core hole, usually referred to as the $K\gamma$ fluorescence spectrum. The spectrum was excited with the incident photon energy at 8460 eV, well above the absorption threshold. There is no detailed calculation of the $K\gamma$ fluorescent spectrum to our knowledge so far. Curve (c) is the inelastic-scattering spectrum measured with the incident photon energy tuned to the peak of the absorption spectrum. Another spectral feature, in addition to the valence-band emission spectrum, appears in the spectrum with energy higher than that of the absorption threshold. The feature can be roughly fitted with two peaks. The energy
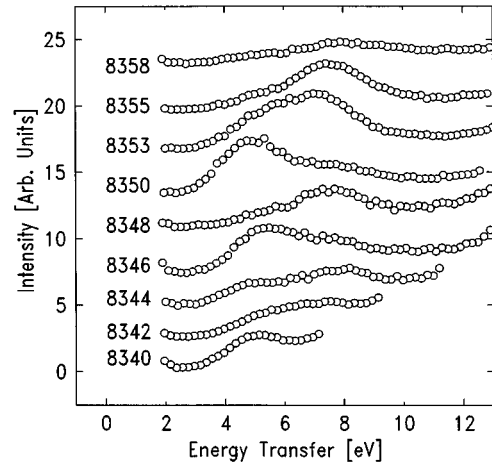

FIG. 2. Resonant inelastic-x-ray-scattering spectra of NiO. The incident photon energy is indicated in the figure.

separations between the two peaks and the elastic line are about 4.9 and 7.8 eV, respectively.

Figure 2 shows a series of inelastic-scattering spectra taken with the incident energy tuned between 8340 and 8360 eV. The scattering intensity is plotted as a function of the energy transfer instead of the scattered photon energy. All spectra in Fig. 2 can also be roughly fitted with two broad peaks with strong variation in peak intensities but nearly constant energy transfers. The energy transfers are centered around 4.9 and 7.8 eV, though small variations of the peak positions with the incident energy is clearly observed. The above observation also indicates that the average scattered photon energy disperses linearly with the incident photon energy, an important characteristic of XRRS. It should be noted that, for incident energies well below the absorption threshold, the only observed loss feature is a broad peak centered between 20 and 25 eV, while for incident energies well above the main absorption peak, there is no observable loss feature in the spectrum at all because of the strong absorption of the sample.

The strong variation of the scattering cross section as a function of the incident energy is better illustrated with con-
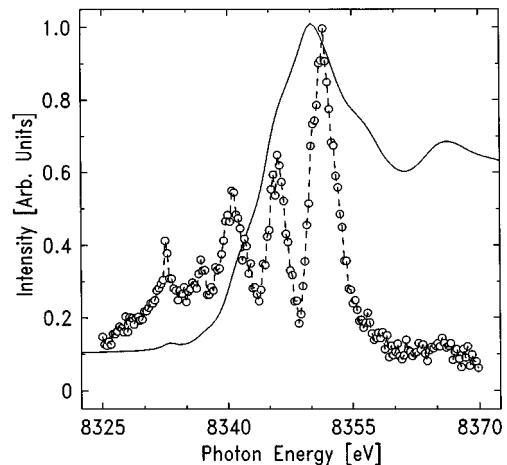

FIG. 3. Constant final-state spectrum obtained with energy transfer set to 5 eV. The Ni K absorption spectrum of NiO is also included for comparison.
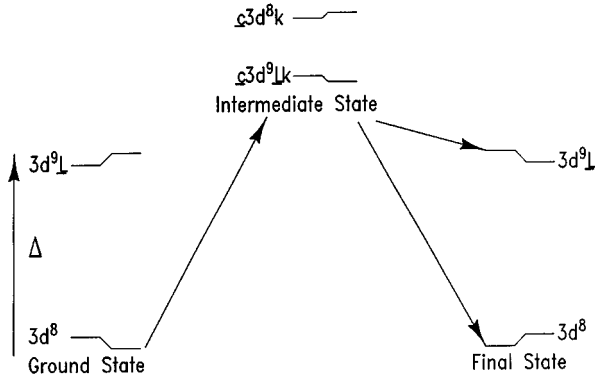
FIG. 4. Schematic energy-level diagrams of NiO in the ground state, the intermediate state, and the final state of the x-ray resonant Raman process.
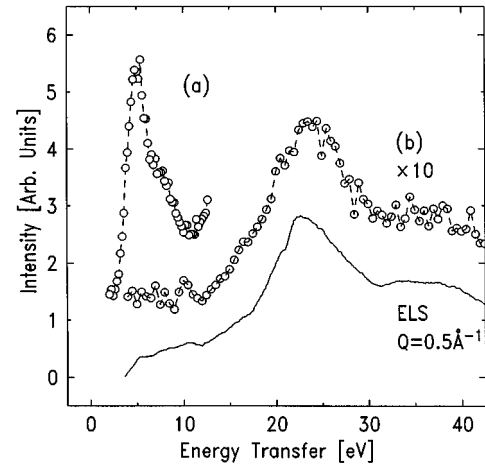

FIG. 5. Resonant enhancement of the scattering cross section: (a) on-resonant spectrum and (b) off-resonant spectrum. Also included is the ELS spectrum of NiO reported by Aryasetiawan *et al.* (Ref. 9).

stant final state scans. In a constant final state scan, both the monochromator energy and the analyzer energy are scanned together, while the energy transfer is kept constant. The intensity variation in a constant final-state scan then represents only the intermediate states that subsequently decay into the particular final states having the energy transfer being monitored. Figure 3 shows a constant final-state scan with the energy transfer kept at 5.0 eV. The Ni K absorption spectrum is also included in the figure for comparison. The constant final-state scan shows a series of resonances in the scattering cross section with resonant energies close to the local maxima in the absorption spectrum. The resonances in the constant final-state scan are also better resolved than their counterparts in the total absorption spectrum.

In the following, the loss feature and its resonant behavior will be interpreted in terms of a cluster model or the Anderson impurity model. This approach was used by Tanaka and Kotani[6] in their theoretical study of resonant soft-x-ray-emission processes and has also been very successful in interpreting a wide range of spectroscopic data on the electronic structure of NiO and other highly correlated systems.[8,12,13] In the cluster description of NiO, in order to account for the covalency between the metal ion and the ligand, the ground state is represented by a linear combination of the following configurations: $3d^8, 3d^9\underline{L}, 3d^{10}\underline{L}^2$, where $\underline{L}$ denotes a ligand hole at the center of the ligand band. The energies of the $3d^9\underline{L}$ and the $3d^{10}\underline{L}^2$ configurations are given by Δ and $2\Delta + U_{dd}$, respectively, where Δ is the anion-to-cation charge transfer energy and U_{dd} the d-d Coulomb interaction energy. The $3d^{10}\underline{L}^2$ configuration will be neglected in the following discussion because its energy is much higher than the other two configurations. The ground state is then the bonding state resulting from the mixing of the $3d^8$ and the $3d^9\underline{L}$ configurations as shown in the schematic in Fig. 4. The intermediate state in the XRRS process is the same as the final state of the x-ray-absorption process, which can be represented by $\underline{c}3d^8k + \underline{c}3d^9\underline{L}k$, where $\underline{c}$ denotes the Ni $1s$ core hole and k the excited photoelectron. The order in energy for these configurations can be rearranged from that of the ground state due to the core-hole–valence-electron Coulomb interaction. In this particular case, from the parameters obtained from other core level spectroscopies, $\underline{c}3d^9\underline{L}k$ is expected to have energy lower than

that of $\underline{c}3d^8k$, which affects the distribution of the spectral weight in the intermediate state in favor of the former. Qualitatively, the lowering of the energy of the $\underline{c}3d^9\underline{L}k$ configuration can be thought of as due to charge screening from the ligand to the metal ion in the presence of the core hole. The intermediate state then decays into the final state through either radiative or Auger processes. In the case of radiative decay, the excited state can decay either by filling the core hole with valence electrons, resulting in the valence-band emission in the presence of a spectator electron, or by direct recombination of the excited electron with the core hole, thus returning the system to either the ground state or the excited $3d^9\underline{L}$ configuration. A schematic of the energetics discussed above is shown in Fig. 4.

The proposed interpretation is supported by the following observations. First, the energy transfer of the loss feature is close to the recently reported charge-transfer energy of NiO, 6.2 eV.[7] It should be noted that charge-transfer energy is typically obtained indirectly from photoemission or x-ray-absorption experiments.[7,8] Second, the excited $3d^9\underline{L}$ state should have a dispersional width comparable to the ligand bandwidth since the Ni $3d$ bandwidth is much narrower and can be neglected. The total width of the loss feature is between 5 and 6 eV, which is slightly broader than the O $2p$ bandwidth of 4 eV determined by angle-resolved valence-band photoemission measurements.[14] The difference in width would be smaller if the difference in energy resolution between the two experiments is taken into account. Third, since the intermediate state in the XRRS process is the final state of the Ni K edge absorption process, absorption maxima in the absorption spectrum should, in principle, coincide with that in the inelastic cross section as shown in Fig. 3 if the appropriate final state is being monitored. However, more model calculations are clearly necessary to account for the detailed line-shape change in the spectra as a function of the incident energy.

Finally, it is interesting to estimate the magnitude of the resonant enhancement of the inelastic scattering cross section. Figure 5 compares the inelastic-scattering spectrum

taken with the incident photon energy tuned to 7920 eV, far below the Ni *K* absorption edge, curve (a), to the spectrum obtained with incident energy tuned to 8350 eV. Also included is the electron energy-loss spectroscopy (ELS) spectrum measured at similar momentum transfer reported recently.[9] Note that far from any absorption edge, the inelastic x-ray scattering and ELS are measuring the same quantity, the dielectric response function of the system. This is illustrated by the similarity between the ELS spectrum and the nonresonant inelastic-x-ray-scattering spectrum. However, there is clearly intensity in the ELS data between 4 and 10 eV energy transfer, which is absent in the nonresonant x-ray data because of the strong absorption in NiO. If one assumes that the same relative intensity between the 4 and 10 eV loss feature and the main loss peak in the ELS data also exists in the nonresonant x-ray spectrum, then the on-resonant inelastic-scattering cross section corresponding to the present loss feature is about 100 times larger than the nonresonant cross section. The enhancement factor would be even higher if one takes into account the self-absorption correction.

In summary, an XRRS study of NiO near the Ni *K* absorption edge was carried out. An energy-loss feature with energy transfer close to the anion-to-cation charge-transfer energy in NiO is observed. A configuration-interaction cluster model of NiO is used to qualitatively interpret the scattering cross section and the strong incident energy dependence. In comparison with other experimental techniques, XRRS may provide a more direct way of studying charge-transfer excitations in many similar, highly correlated systems. Furthermore, large resonant enhancement of the inelastic-scattering cross section is observed. This is very important in applying high-resolution inelastic x-ray scattering to high-*Z* materials because of the strong sample absorption.

[1] See, for example, R. Loudon, *The Quantum Theory of Light* (Oxford University Press, New York, 1973), Chap. 8.

[2] C. J. Sparks, Jr., Phys. Rev. Lett. **33**, 262 (1974).

[3] See, for example, P. Eisenberger *et al.*, Phys. Rev. Lett. **36**, 623 (1976); K. Hamalainen *et al.*, *ibid.* **67**, 2850 (1991); V. Etelanium *et al.*, J. Phys., Condens. Matter **4**, 879 (1992); M. Krisch *et al.*, Phys. Rev. Lett. **74**, 4931 (1995).

[4] See, for example, J.-E. Rubensson *et al.*, Phys. Rev. Lett. **64**, 1047 (1990); Y. Ma *et al.*, *ibid.* **69**, 2598 (1992); W. L. O'Brien *et al.*, *ibid.* **70**, 238 (1993).

[5] Y. Ma *et al.*, Phys. Rev. Lett. **74**, 478 (1995); Y. Ma and M. Blume, Rev. Sci. Instrum. **66**, 1543 (1995).

[6] S. Tanaka and A. Kotani, J. Phys. Soc. Jpn. **62**, 464 (1993).

[7] Geunseop Lee and S.-J. Oh, Phys. Rev. B **43**, 14 674 (1991); J. van Elp, H. Eskes, P. Kuiper, and G. A. Sawatzky, *ibid.* **45**, 1612 (1992).

[8] G. A. Sawatzky and J. W. Allen, Phys. Rev. Lett. **53**, 2339 (1984).

[9] F. Aryasetiawan, O. Gunnarsson, M. Knupfer, and J. Fink, Phys. Rev. B **50**, 7311 (1994).

[10] C.-C. Kao, K. Hamalainen, M. Krisch, D. P. Siddons, T. Oversluizen, and J. B. Hastings, Rev. Sci. Instrum. **66**, 1699 (1995).

[11] See, for example, Z. Tan, S. M. Heald, S.-W. Cheong, A. S. Cooper, and A. R. Moodenbaugh, Phys. Rev. B **47**, 12 356 (1993).

[12] J. Zaanen, G. A. Sawatzky, and J. W. Allen, Phys. Rev. Lett. **55**, 418 (1985).

[13] A. Fujimori and F. Minami, Phys. Rev. B **30**, 957 (1984).

[14] Z.-X. Shen, C. K. Shih, O. Jepsen, W. E. Spicer, I. Lindau, and J. W. Allen, Phys. Rev. Lett. **64**, 2442 (1990).